

Influence of Operating Parameters on Pyramid Solar Still with Phase Change Material (PCM)

D. Srinivas* , Gupta AVSSKS **† 

* Research scholar, Centre for Energy Studies, JNTU College of Engineering, Kukatpally, HYDERABAD-500085

** Professor, Department of Mechanical Engineering, JNTU college of Engineering, Kukatpally, HYDERABAD-500085

(dharamsothsrinivas@gmail.com, avs_gupta@rediffmail.com)

†

D. Srinivas; Gupta, AVSSKS, JNTU College of Engineering, Kukatpally, HYDERABAD-500085,
 dharamsothsrinivas@gmail.com

Received: 22.07.2021 Accepted: 18.08.2021

Abstract- In the recent scenario, distillation with solar still plays a vital role in obtaining potable water from brackish and sea water. The inspiration for this paper is the partial availability of clean water resources and the plenty of availability water due to potential renovation into filtered water using solar energy. In this paper, an attempt is made to study the productivity of pyramid solar still. To achieve this goal, a distillation system was fabricated which incorporates a square pyramid fiber glass placed on a black coated Aluminum basin. The solar radiation, which is incident on the black coated basin heats up the water and evaporates it forming vapors onto the fiber glass cover which is condensed to potable water. For analyzing the performance of still, the distillation system is operated at different water depths viz; 5 cm and 10 cm, along with paraffin wax material and preheated water, The experimental setup is placed at an angle of 50 degree to the horizontal. The hourly productivity is higher in case of solar still with PCM during sunny days. From the experimental analysis, it is observed that there is 75% increase in the efficiency of still, when operated with PCM, at 5 cm depth of water.

Keywords Solar still, Desalination, square pyramid, Sustainability, Phase change Material (PCM).

Nomenclature

q_{ew} : Rate of evaporative heat transfer from water surface to glass (W/m ²) h_{cw} : Convective heat transfer coefficient from water to glass (W/m ² OC) h_e : Evaporative heat transfer coefficient from water to glass (W/m ² OC) m_w : Yield of water per unit area per hour from distiller (kg/m ² /hr)	p_w : Partial vapor pressure at water temperature (N/m ²) p_g : Partial vapor pressure at glass temperature (N/m ²) K : Thermal Conductivity of Al (W/m ² K) d : Average spacing between the water surface and the fiber glass (m) L : Latent heat of vaporization of water = 2260 kJ/kg	PCM: Phae Change Material SHS : Sensible Heat Storage WHS: Workable Heat Storage SPC:Solar Parabolic Concentrator $I(t)$: Amount of solar radiation within a given time interval (W/m ²) η_s : Efficiency of solar still (%) T_w : Water temperature (OC) T_g : Glass temperature (OC) T_a : Ambient temperature (OC)
--	---	---

1. Introduction

Distillation technology is used for almost a period in land plants and on craft to supply water to a bunch [1]. Distillation is one of the numerous processes accessible for water “distillation” and “sunlight” is form of thermal energy is used to conduct this development [2]. Daytime has the advantage of taking a zero-fuel cost, but wants additional gap (for its gathering) and still has to be temperately clean [3]. The solar still considered and verified widely for the making

of purified lwater using solar energy. In maximum cases, even under enhanced working state, the acknowledged \$efficiency of osingle-basin solar system was between 30% and 45.5%, with less than 5l/ m² / day of fresh \$water making [4]. This llow productivity for the most part is because of the entire loss of still tenderness of build-up of water steam on sun oriented still glass cover [5]. The main disadvantage of the solar desalination by means of solar stills is its low efficiency and creation rate[19]. Generally, a solar still can produce 2.5–5 l/m²/day of distillate. Nevertheless,

solar distillation is a modest method, efficiency seems to be low due to the huge thermal size and ingesting of time. Multi impact sun powered stills were utilized to enhance generation of desalinated water however just in little limits, this is on the grounds that %condenser is an essential piece of the still [6, 7]. The small heat and mass move ccoefficients in this moderate of still want activity at moderately high “temperatures”, therefore the utilization of extensive, costly, brass %surfaces for dissipation and build up [8, 9]. A sun oriented still, with its lower profitability, does not rival other desalination procedures. In any case, the request of crisp water does not surpass a couple of cubic meters, the sun based still is an accessible choice [10]. Solar stills utilize the very same procedures that happened in nature that creates precipitation, specifically vanishing and build up. The sun based still development can be effectively portrayed as takes after; a straightforward cover encases a dish of salty water; this development warms up the water instigating vanishing and builds up on inward face of inclining straightforward cover [11, 12]. The shaped refined water is for the most part consumable; the nature of the distillate is high since every one of the salts, inorganic and natural segments and

organisms are abandoned in the shower. Amid sensible states of daylight, the temperature of water will increase adequately to kill every pathogenic bacterium in any case. A layer of ooze is probably going to create in the base of the tank and ought to be flushed out as regularly as important [13, 14]. Keeping in mind the end goal to evaporate 1kg of water at ‘temperature’ of 30oC around 2.4×10^6 J is mandatory. For a sun orient radiation of 250 W/m², amid a found the middle value of time of 24h, this energy might evaporate a most extreme of 9 l/m²/day. By and by, and because of the heat calamity, the normal efficiency from the sunlight based still is in the assortment 452/m²/day. The present best in class single-impact sun powered stills have a proficiency of around 30% to 40%. The day-by-day measure of drinking water required by people alterations between 2L and 8L for every individual and the run of the mill necessity for refined water is 5L for each individual every day, henceforth roughly 2m² of still are required for every individual served [15]. Schematic of Pyramid solar distillation scheme is shown in Fig.1



Fig. 1. Schematic of Square Pyramid solar distillation system.

2. Phase Changing Materials (PCM)

PCM is a material which melting and hardening at firm temperature, is accomplished of loading, emancipating immense quantities of energy[15]. Heat is captivated while substantial deviations after solid to liquid then heat is enlightened while the substantial changes from liquid to solid. Henceforth, PCM’s are similarly so-called a covert heat storing systems. The solar energy was conveyed through glass cover, was captivated by PCM and basin, hence these temperatures rise. Nearly part of the energy

was shifted to basin water by convection and the outstanding was moved to the PCM by conveyance. paraffin series wax balls are ‘heated’, the heat is kept as workable heat up until PCM spreads its ‘melting’ point. Functional heat is the quantity of energy that is typically riveted or released by a substance during a change in temperature. PCM flinches to melt after comprehensive melting of PCM, heat is kept in the melted PCM as a workable heat. Once the solar radiation flinches to reduction the workings of still flinches to cool [16]. PCM handovers heat to sink liner and there to the basin water till

PCM hardens totally. That PCM performances as temperature basis throughout less sunlight times also flat at darkness [17]. Still endures to harvest fresh water even night. Fluid gas phase changes are not applied to usage like thermal stowage due to the big capacities or high burdens essential to store the resources when in gas phase. liquid gas evolutions do have a developed heat of conversion than solid liquid conversions [18][20]. SPC are classically very sluggish, have a somewhat low heat of alteration. Originally, the solid fluid PCM's perform comparable workable heat storage (WHS) resources; temperature increases as they captivate temperature. Dissimilar conformist SHS, still, while PCMs influence the ttemperature at which change pphase by captivate in large quantities of heat at nearly persistent temperature. PCM remains to captivate heat deprived of important rise in ttemperature till all the substantial is altered to the fluid phase. while the ambient ttemperature around a liquid mmaterial falls, PCM congeals, discharging its kept latent hheat. A huge amount of PCMs are accessible in any essential temperature variety from 50oC to 190oC. Inside the human comfort choice, which is among 203oC, some PCM's are actual operative[21]. They supply 5 to 10 times more heat/unit volume than predictable storage supplies such as lwater, mmasonry or rock. Solar still's efficiency was 58% and 51% for the lstill with, without PCM[22].

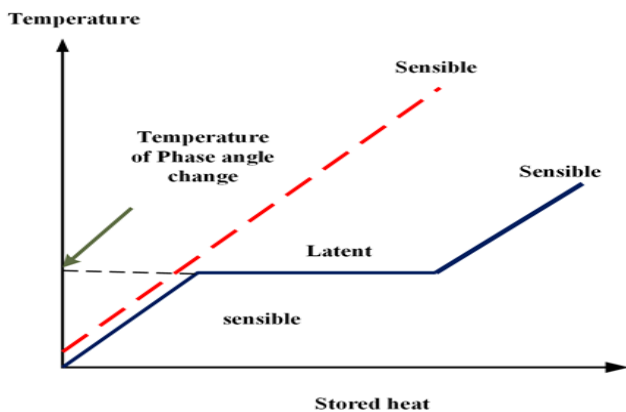


Fig. 1. Sensible heat storage in PCM.

3. Mathematical Modelling

The solar radiation intensity data can be found from the pyranometer reading, from which the output is in millivolts and then required value of intensity can be obtained by using the formula:

$$I(t) = 154.5 \times (I_b - 3.2) \text{ W/m}^2 \quad (1)$$

The rate of heat transfer per unit area from the water surface to the glass cover can be obtained from equations defined by Medugu and Ndatuwong et al., 2009. Thus, the

hourly evaporation per m2 from the solar still is calculated by the equation:

$$\dot{q}_{ew} = 0.016 \times h_{cw} \times (p_w - p_g) \text{ W/m}^2 \quad (2)$$

$$\dot{q}_{ew} = h_{ew} \times (T_w - T_g) \text{ W/m}^2 \quad (3)$$

The convective heat transfer coefficient is calculated by the equation,

$$h_{cw} = 0.016 \times h_{cw} \times \frac{(p_w - p_g)}{(T_w - T_g)} \quad (4)$$

The evaporative heat transfer coefficient is calculated by the equation,

$$h_{cw} = 0.884 \times \left[T_w - T_g + \frac{(p_w - p_g) \times T_w}{268.9 \times 10^2 - p_w} \right]^{\frac{1}{3}} \quad (5)$$

The values of p_w and p_g are obtained from the following expression (for the range of temperature (10° C -90° C) .

$$P(T) = \exp \left(25.317 - \frac{5144}{T+273} \right) \quad (6)$$

The hourly distillate output per m² or yield of the still per unit area per hour (kg/m²/hr) from a distiller unit is given by the following equation:

$$\dot{m}_w = \frac{\dot{q}_{ew}}{L} \times 3600 \quad (7)$$

$$\dot{m}_w = 0.0163 \times (p_w - p_g) \times \frac{k}{d} \times 3600 \quad (8)$$

Efficiency of the solar still is given by,

$$\eta_{still} = \frac{\dot{q}_{ew}}{I(t)} = \frac{(\dot{m}_w \times L)/3600}{I(t)} = \frac{h_{ew} \times (T_w - T_g)}{I(t)} \times 100 \quad (9)$$

Efficiency of the solar still is given by,

$$\eta_{still} = \frac{\text{mass of water} \times \text{Latent heat of vaporization of water}}{\text{average solar radiation} \times \text{no. of hours} \times \text{time(sec)}}$$

A pyramic cut-glass solar still project with gatherer area of 1.21m² (1.10m,1.10 m) is presented as demonstrated in Fig.4 and 5. The still is occupied with salty water to elevation of 0.05m. The financial point of opinion, the solar still with saw dust protecting substantial has less cost of production[23]. Therefore, the price of fresh water making is less. In the opinion of ecological substantial, saw dust would be a good substitute for glass wool. The water stowage basin of the still is made with length 0.95m,0.95m 0.10m of minor steel. The water stowage section is providing of width 0.90m, and the residual 0.05m is permitted for the water gathering section.

4. Experimental Setup

Fabrication of the square pyramid solar still includes four stages:

- 1) Metal basin construction and its piping
- 2) Square pyramid fibre glass assembly
- 3) Wooden box fabrication

4) Catchment channel

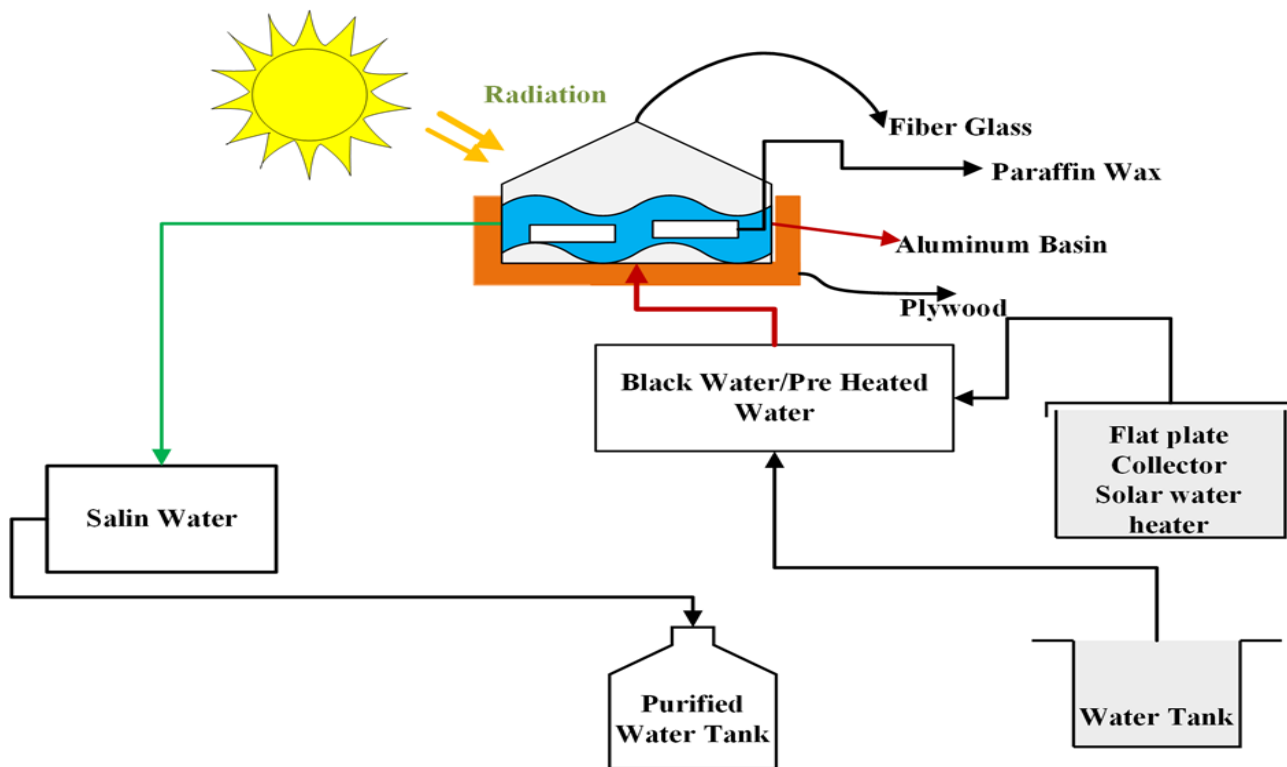


Fig. 3. Block diagram of Square Pyramid solar distillation system.

4.1. Metal basin construction

Aluminium material of 9mm gauge has been chosen for the construction of the metal basin for its good thermal conductivity of 205 W/mK, which allows the maximum solar energy conversion to heat that suffice the rate of evaporation of water as shown in Fig.3. The design dimensions are cut and the metal sheet is hammered and welded in to a square shaped basin of 70 cm × 70 cm i.e., 1 m² with a height of 15 cm and a step of 2 cm is made at its top for the square pyramid glass placement. Two circular sections of diameter 1.5 cm are welded in to the Al basin on opposite corners of a diagonal for inlet and outlet piping respectively. For maximum captivation of solar energy and to reduce the reflective nature of the basin, the basin is layered inside with the black paint and is dried for 2 days for its complete adhesion to Al basin.



Fig. 4. Block diagram of Square Pyramid solar distillation system.



Fig. 5. Black coated Aluminium basin

The maximum water storage capacity of the basin is 64 litres. But, for the efficient operation of the still, as the

water depths are restricted to a maximum of 10 cm and below, the maximum allowable fill is 16 litres.

The average temperature attained by the basin during sunny hours of the day is 59 °C, which suffice the rate of evaporation of water.

The outer section of the metal basin is completely coated white so that the radiative losses out from the basin are minimized and the outer edges are coated black which heats up so that there is an upward movement of airflow which may possibly increase the condensation rate, as glass temperature reduces.

4.2. Square pyramid fiber glass design

The fibre glass sheet is cut in to four equilateral triangular sheets of similar dimensions as shown in Photograph 4.3, relative to Al basin for the pyramid to fit on the basin. The pyramid shape is formed by placing the four triangular sheets on the square of the basin, which inclines with a slope of 50°. Silicone sealant and adhesives are used to glue the four triangular sheets. Four Al L-bends are fitted on to the four sides of the pyramid joints and glued for increasing the mechanical strength. L-bends are also bolted on the base of the pyramid and sealed with silicone sealant.



Fig.6. Fiber glass sheet cut into 4 triangular faces forming the square pyramid

A square wooden frame is constructed and then the L-bends at the base of the square pyramid is bolted in to the wooden frame and sealed, so that the square pyramid fits tightly into the Al basin. Rubber strips are glued on to the four sides of the wooden frame and are also provided on to the Al basin, so that the leakage of vapours is avoided.



Fig. 7. Wooden frame and Al-bends bolted to fiber glass
4.3. Wooden box

Aluminum basin, integrated with the tightly sealed square pyramid fiber glass is placed in the wooden box. Plywood of 20 mm thickness is used to fabricate a wooden box of length 73 cm × 73 cm and a height of 12 cm. Grooves are provided on either sides of the piping sections respectively. A gap of 3 cm thickness is left between the Al basin and the wooden box for placing the thermal storage materials for latent heat and can also be used to place insulating, materials for enhancing the productivity of the still.



Fig. 8. Wooden box for square pyramid solar still

4.4. Catchment channel

Rectangular wall wiring electric conduits of 2 cm wide are used for the construction of catchment channel. The conduit has the following properties:

- low wettability
- high thermal resistance
- non-toxic
- low temperature coefficient of expansion

The catchment channel is fitted onto the base of the square pyramid which slopes down from all the corners to outlet corner for the condensate to flow down to the outlet section.

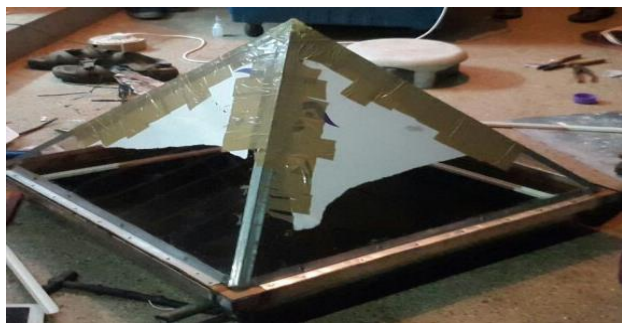


Fig. 9. Catchment channel inside the still

Table 2: Tolerance Limits of Measuring Devices

No	Device	accurateness	range	Error
1	IR Thermometer	$\pm 0.1\text{ }^{\circ}\text{C}$	0-100 $^{\circ}\text{C}$	5%
2	Pyranometer	$\pm 1\text{ W/m}^2$	0-1400 W/m^2	2.5%
3	Measuring jar	$\pm 10\text{ ml}$	0-1000 ml	10%
4	Data logger	$\pm 0.15\text{ }^{\circ}\text{C}$	0-150 $^{\circ}\text{C}$	7.5%

Table 3: Temp. Vs Time(hr)

Time(h)	$T_B(^{\circ}\text{C})$ Temp. of basin	$T_w(^{\circ}\text{C})$ Temp. of water	$T_s(^{\circ}\text{C})$ Temp. of steam	$T_g(^{\circ}\text{C})$ Temp. of glass in side	$T_g(^{\circ}\text{C})$ Temp. of glass out side	$T_a(^{\circ}\text{C})$ Temp. of ambient
08:00	25.3	26.5	26.5	27.6	22.2	32.4
09:00	29.5	28.8	29.3	29.5	23.5	34.8
10:00	34.8	34.3	34.2	36.4	25.1	36.2
11:00	39.4	42.5	39.8	39.8	26.8	38.8
12:00	46.5	51.4	46.1	48.2	27.7	40.5
13:00	50.4	54.6	51.7	52.3	32.4	41.3
14:00	51.6	56.4	52.9	54.8	32.4	43.8
15:00	48.4	50.4	49.6	49.5	31.7	43.2
16:00	39.5	39.5	36.5	42.8	26.2	42.8
17:00	34.4	27.3	32.4	36.4	24.5	42.5
18:00	29.3	25.3	29.6	29.8	21.5	40.6

5. Experimental Procedure

Water is filled inside the solar still through a water supply. A float is present inside the trough which automatically closes the valve after it reaches the required level. A measured quantity of energy absorbing material is added. Two thermocouples are placed inside the solar still in order to measure the temperatures at various locations and at various instants of time. The solar still is covered with a glass cover. The solar radiation passes through the glass cover. A major portion of this solar radiation is absorbed by the black painted surface of the basin generally known as black liner. Concentration of solar radiation is restrained through a device known as pyranometer. With the help of this, setup temperature is recorded for every half an hour using the temperature indicator and the intensity is noted by using pyranometer. The readings are noted from sun rise to sun set.

6. Results and Discussions

The experiment is conducted on May 25th 2020, from 8.A.M to 6.P.M.

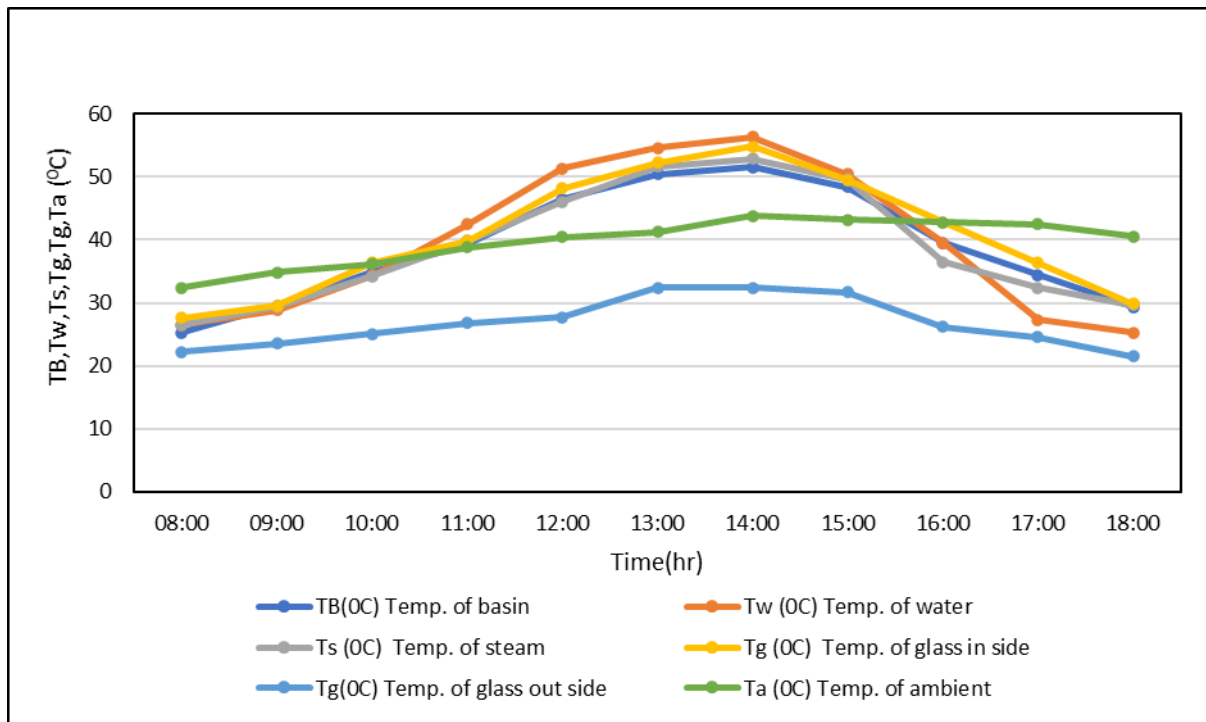


Fig. 10. Temperature variation in different components with 5cm water depth

Table 4: Partial vapor pressure at water temperature (N/m^2), Partial vapor pressure at glass temperature (N/m^2) V with Time(hr)

Time(h)	Pg (w/m ²)	Pw (w/m ²)
08:00	2674.52	3434.77
09:00	2886.86	3915.11
10:00	3168.6	5311.64
11:00	3494.32	8206.82
12:00	3678.45	12836.31
13:00	4786.31	14986.78
14:00	5056.79	16329.49
15:00	4604.64	1222.1
16:00	3376.13	7017.76
17:00	3060.22	4759.98
18:00	2566	3205.47

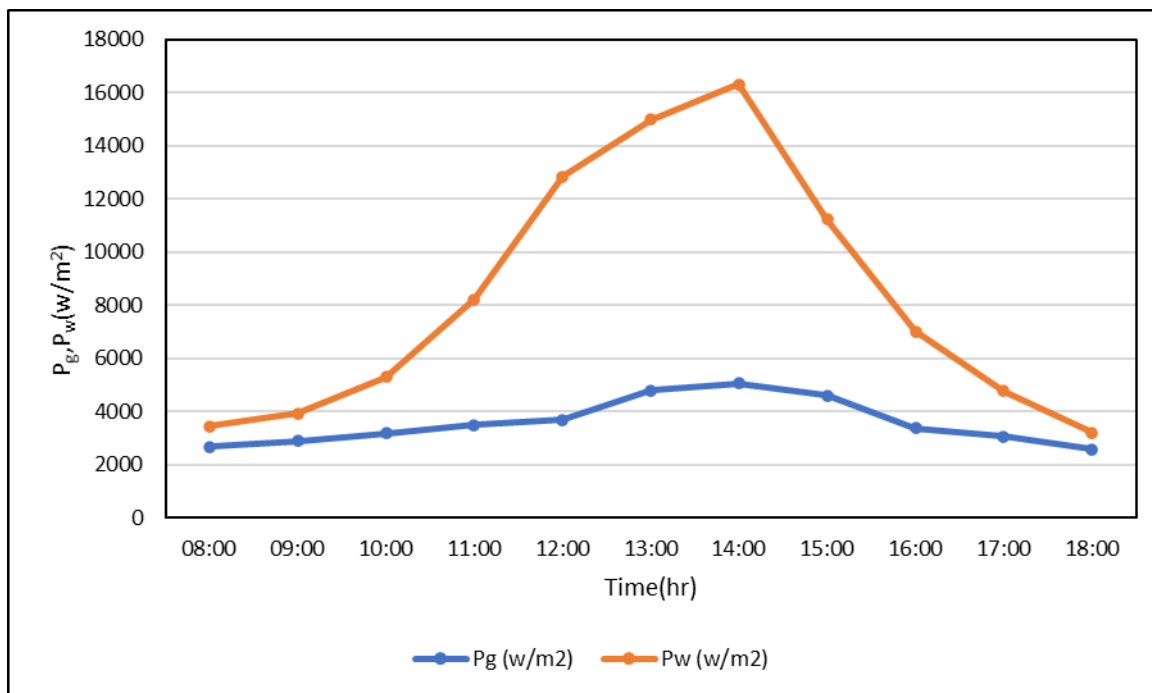


Fig. 11. Results of Partial vapor pressure at water temperature (N/m^2), Partial vapor pressure at glass temperature (N/m^2) Vs Time(hr) with 5cm water depth

Table 5: Convective heat transfer Coefficient from water to glass ($W/m^2 C$), Evaporative heat transfer Coefficient from water to glass ($W/m^2 C$) with Time(hr)

Time(h)	hcw (w/m2)	hew (w/m2)	Mw (kg/m2/hr) Mass of water
08:00	1.4459	4.0902	0.028
09:00	1.552	4.0902	0.0416
10:00	1.8708	6.9725	2.8383
11:00	2.249	10.8009	7.503
12:00	2.6032	16.0943	0.0168
13:00	2.5637	18.8475	0.6665
14:00	2.5231	19.7858	0.7248
15:00	2.4073	15.6898	0.4673
16:00	2.1228	9.2997	0.197
17:00	1.7685	6.1662	0.0766
18:00	1.3868	3.7339	0.0226

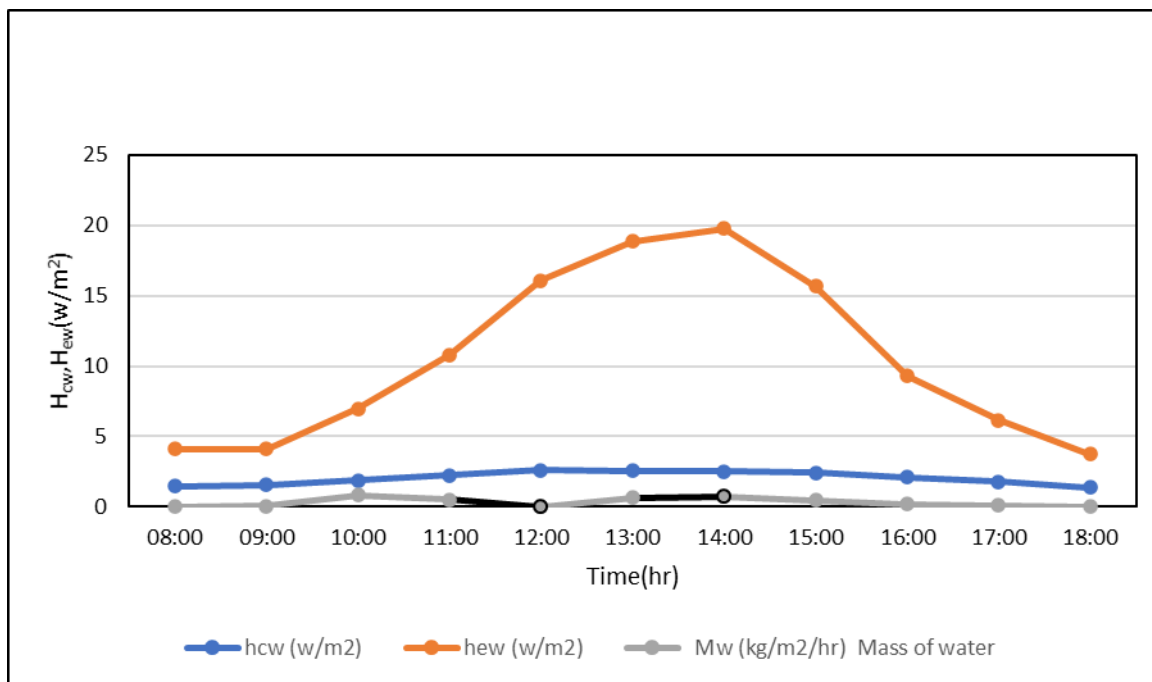


Fig. 12. Results of Convective heat transfer Coefficient from water to glass (W/m^2C), Evaporative heat transfer Coefficient from water to glass ($W/m^2 C$) Vs Time(hr) with 5cm water depth

Table 6: Efficiency of solar still (%) Vs $t_w-t_g/l(t)$

Efficiency (%)	$t_w-t_g/l(t)$ (w/m^2)
7.71	0.0511
8.81	0.0391
11.59	0.014
26.91	0.269
48.65	0.4865
51.29	0.5133
54.76	0.5476
38.91	0.3896
23.03	0.2303
18.56	0.1856
13.64	0.1364

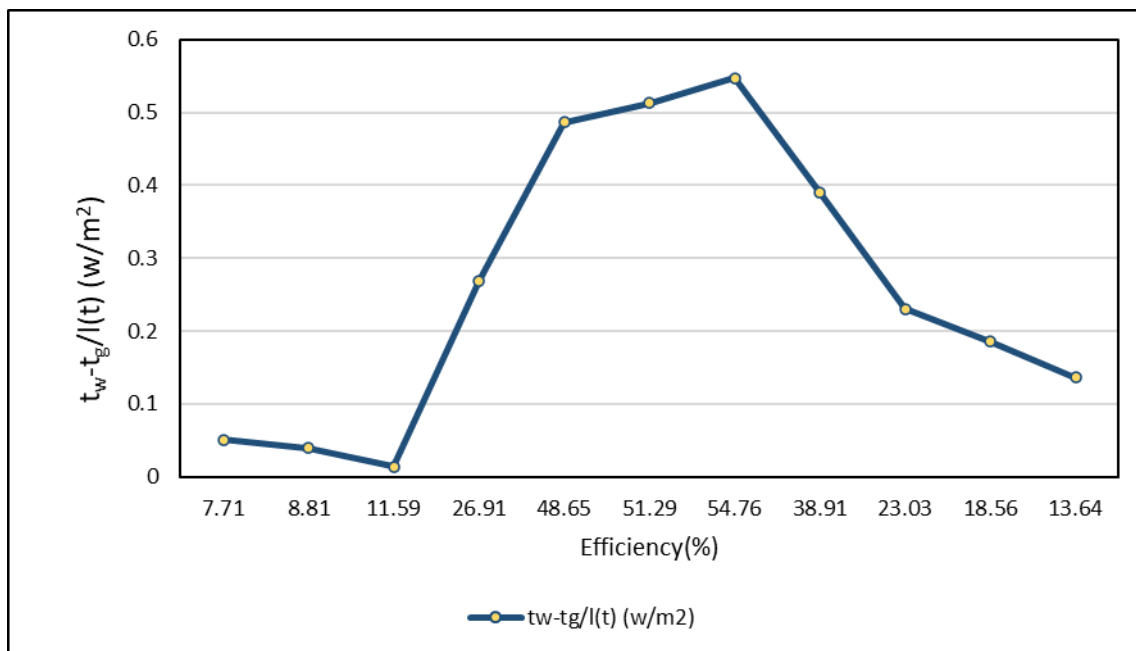


Fig. 13. Results of efficiency of solar still (%) Vs $t_w - t_g / l(t)$ with 5cm water depth

Table 7: various Temp. Vs Time(hr)

Time(h)	T _B (°C) Temp. of basin	T _w (°C) Temp. of water	T _s (°C) Temp. of steam	T _g (°C) Temp. of glass in side	T _g (°C) Temp. of glass out side	T _a (°C) Temp. of ambient
08:00	24.3	22.3	25.4	26.5	25.4	35.4
09:00	28.5	23.9	28.3	29.5	28.8	39.8
10:00	33.8	36.9	33.2	36.4	29.3	39.2
11:00	38.4	40.2	38.8	39.8	30.4	40.8
12:00	45.5	46.5	45.1	48.2	32.7	40.5
13:00	49.4	52.7	51.7	52.3	33.6	41.3
14:00	50.6	55.2	52.9	54.8	36.2	41.4
15:00	47.4	48.9	48.6	49.5	30.7	40.2
16:00	38.5	39.8	35.5	42.8	26.9	41.8
17:00	34.4	29.6	32.4	36.4	22.1	40.5
18:00	28.3	25.4	29.6	29.8	21.4	39.6

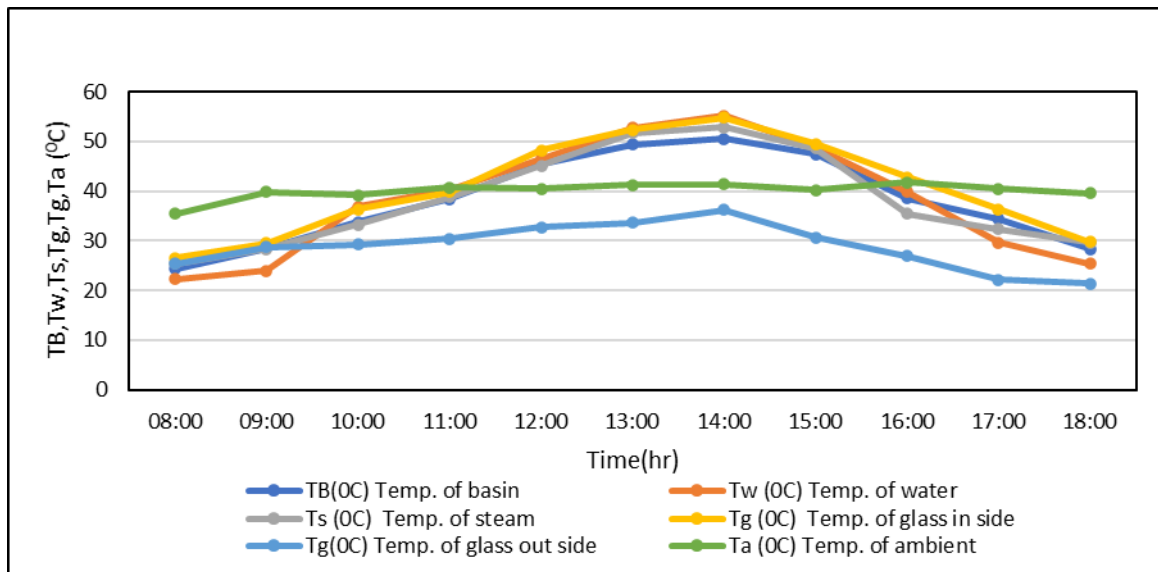


Fig. 14. Temperature variation in different components with 10cm water depth

Table 8: Partial vapor pressure at water temperature (N/m²), Partial vapor pressure at glass temperature (N/m²) Vs Time(hr)

Time(h)	Pg (w/m ²)	Pw (w/m ²)
08:00	3224.05	2690.35
09:00	3915.11	2955.13
10:00	4027.05	6112.53
11:00	4292.9	7280.75
12:00	4866.08	10065.24
13:00	5112.47	13675
14:00	5887.09	15423.23
15:00	4355.66	11348.96
16:00	3514.37	7129.43
17:00	2658.77	4095.56
18:00	2550.82	3224.05

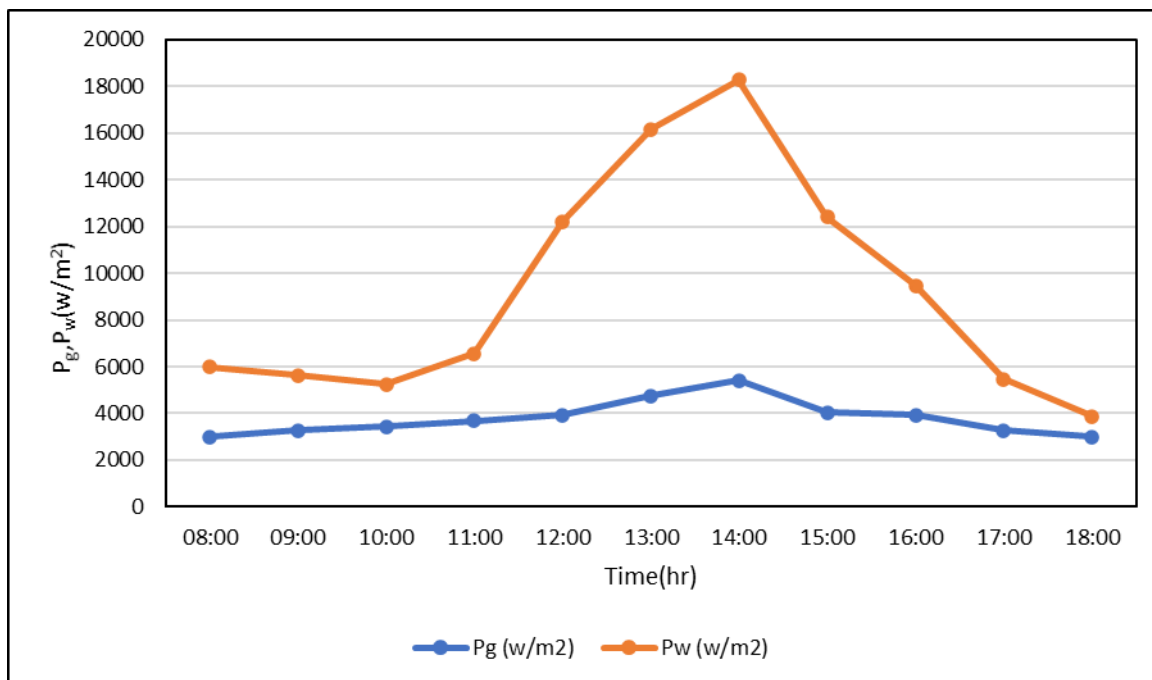


Fig. 15. Results of Partial vapor pressure at water temperature (N/m²), Partial vapor pressure at glass temperature (N/m²) Vs Time(hr) with 10cm water depth

Table 9: Convective heat transfer Coefficient from water to glass (W/m²C), Evaporative heat transfer Coefficient from water to glass (W/m² C) Vs Time(hr)

Time(h)	hcw (w/m ²)	hew (w/m ²)	Mw (kg/m ² /hr) Mass of water
08:00	1.2951	3.5674	0.0176
09:00	1.5102	4.7339	0.0369
10:00	1.7601	7.7272	0.0935
11:00	1.9208	9.3698	0.1462
12:00	2.1671	13.0633	0.2871
13:00	2.4337	17.4564	0.531
14:00	2.4418	19.6087	0.5934
15:00	2.3805	14.6352	0.4242
16:00	2.1022	9.4258	0.1936
17:00	1.7426	5.3413	0.0638
18:00	1.4107	3.7989	0.0242

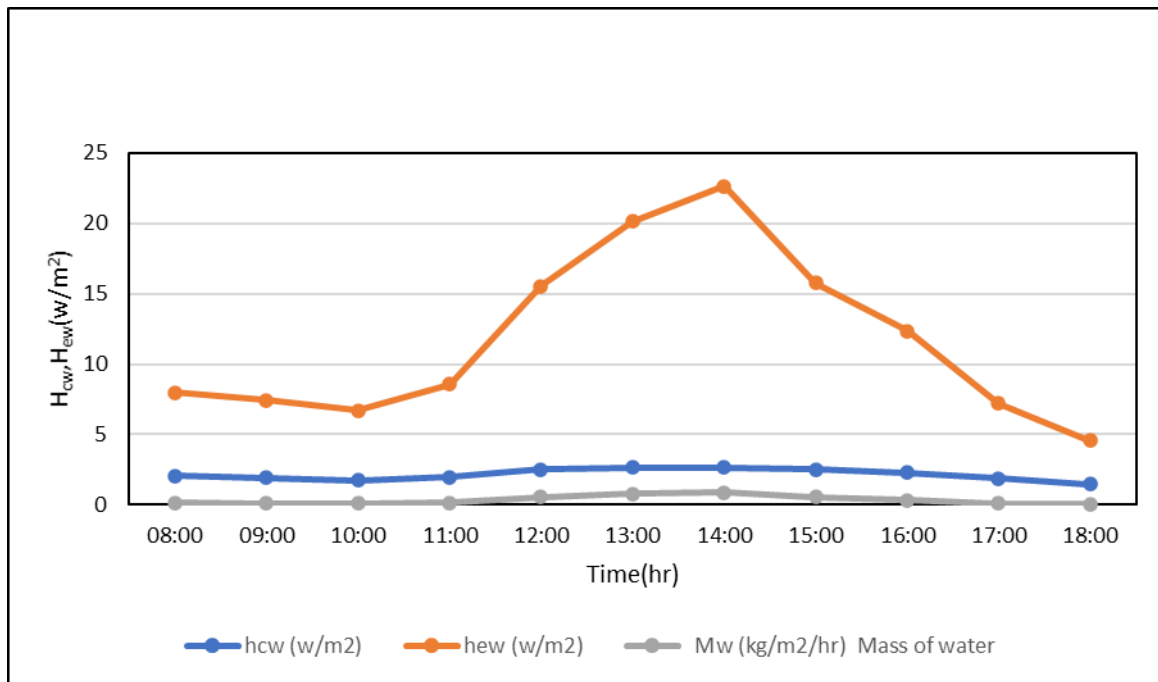


Fig. 16. Results of Convective heat transfer Coefficient from water to glass (W/m^2 C), Evaporative heat transfer Coefficient from water to glass (W/m^2 C) Vs Time(hr) with 10cm water depth\ Table 10: Efficiency of solar still (%) Vs $t_w-t_g/l(t)$

Efficiency (%)	$t_w-t_g/l(t)$ (W/m^2)
5.16	0.0516
7.88	0.0788
11.42	0.1142
14.32	0.1462
22.70	0.2270
40.90	0.4090
45.99	0.4947
35.84	0.3584
22.64	0.2264
16.41	0.1641
13.94	0.1394

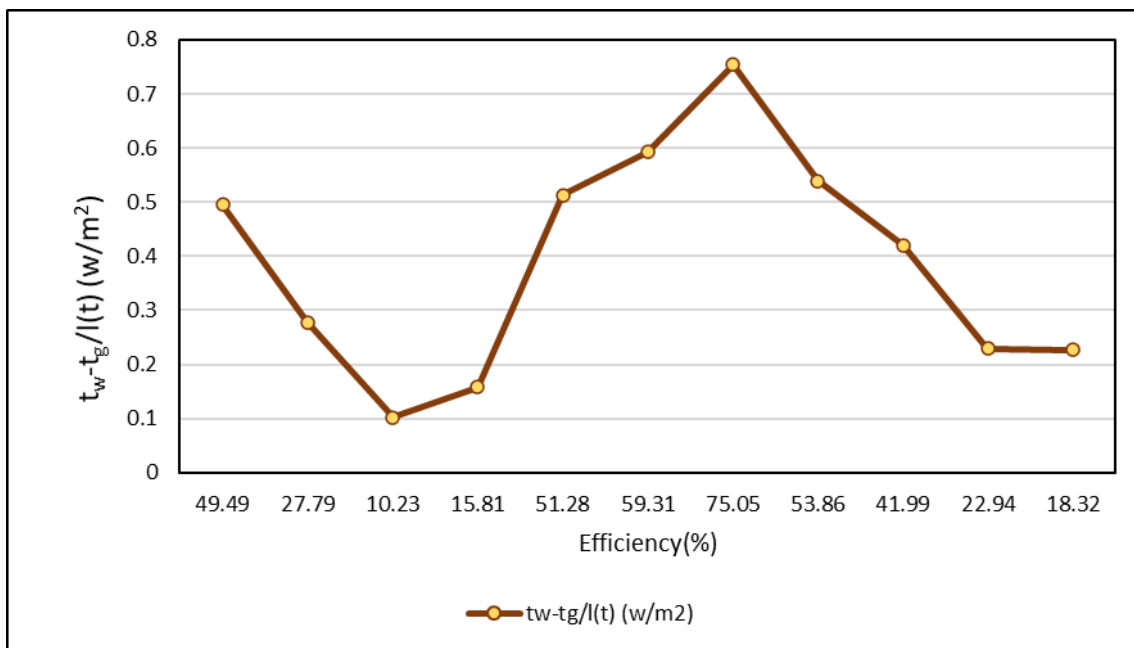


Fig. 17. Results of of Efficiency of solar still (%) Vs $t_w-t_g/l(t)$ with 10cm water depth

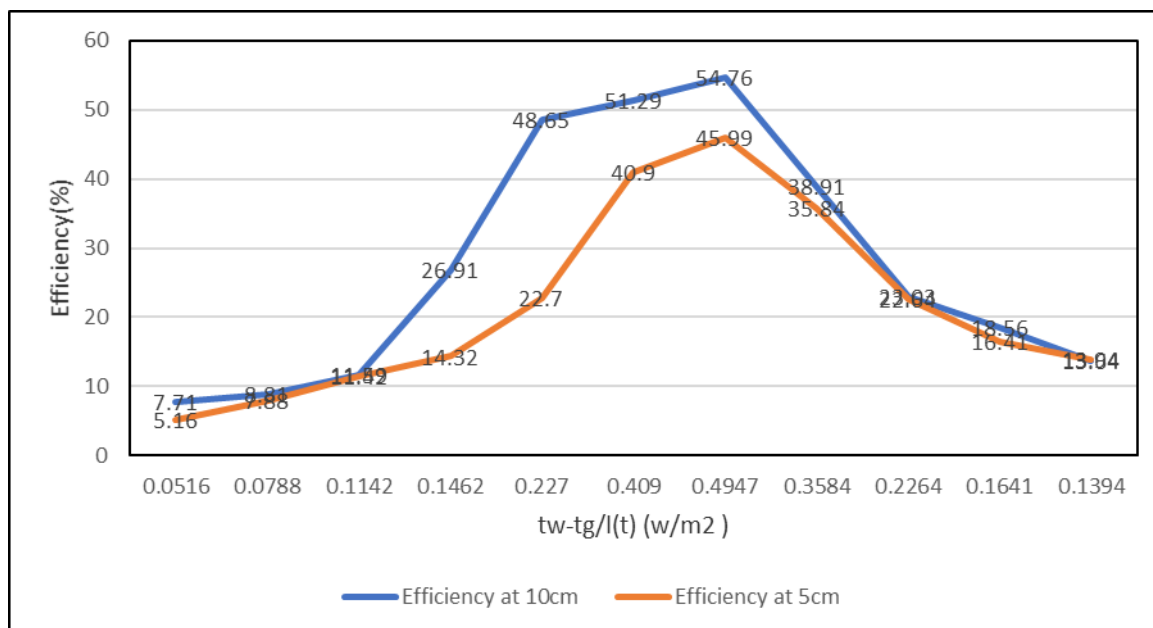


Fig.18.Camapriion Result of Efficiency at 10cm and 5cm water depth.

Table 11: Output Values for a Square Pyramid Solar Still

	Depth of water level (cm)	Water output (0.95m ²) (liters/day)	Total amount of water yield (liters/m ² /day)	Efficiency (%)
Still (preheated water and with PCM)	5 cm	1.28	2.56	54.76
	10 cm	1.08	2.16	45.99

7. Conclusions

The proposed strategy of square pyramid solar still with phase changing material shows great potential in terms of higher distillation yield per unit area. The presentation of the solar still was studied experimentally with respect to latent heat storage and different water depths. The condensed water collected without PCM and with PCM are 2.16 liters/m²/day/10cm with still alone and 2.56litres/m²/day/5cm with still correspondingly. Efficiency of 'still' with PCM is 45.99% for 10cm depth and 54.76% for 5cm depth respectively. There is 75% increase in the efficiency of the solar still when the water depth is decreased. Initially, the solar still is operated without PCM at a water depth of 10cm. To enhance the productivity, the solar still was integrated with PCM and water depth decreased to 5cm. There is 75% increase in efficiency of solar still with PCM at 5cm water depth, by its aiding effect on the evaporation rate of solar still. The distillate yield of the still is 2.56liters/m²/day, when the temperature gradient between the basin liner and the glass cover is high.

References

- [1] I. Al-Hayeka and O. O. Badran, "The effect of using different designs of solar stills on water distillation," *Desalination*, vol. 169, no. 2, pp. 121-127, 2004.
- [2] D. D. W. Rufuss, S. Iniyan, L. Suganthi, and P. Davies, "Solar stills: A comprehensive review of designs, performance and material advances," *Renewable and sustainable energy reviews*, vol. 63, pp. 464-496, 2016.
- [3] Z. Haddad, A. Chaker, and A. Rahmani, "Improving the basin type solar still performances using a vertical rotating wick," *Desalination*, vol. 418, pp. 71-78, 2017.
- [4] A. Kabeel and M. Abdelgaied, "Improving the performance of solar still by using PCM as a thermal storage medium under Egyptian conditions," *Desalination*, vol. 383, pp. 22-28, 2016.
- [5] S. S. Narayanan, A. Yadav, and M. N. Khaled, "A concise review on performance improvement of solar stills," *SN Applied Sciences*, vol. 2, no. 3, pp. 1-15, 2020.
- [6] V. Vigneswaran, G. Kumaresan, B. Dinakar, K. K. Kamal, and R. Velraj, "Augmenting the productivity of solar still using multiple PCMs as heat energy storage," *Journal of Energy Storage*, vol. 26, p. 101019, 2019.
- [7] D. Krishna, M. Sasikala, and V. Ganesh, "Mathematical modeling and simulation of UPQC in distributed power systems," in *2017 IEEE International Conference on Electrical, Instrumentation and Communication Engineering (ICEICE)*, 2017: IEEE, pp. 1-5.
- [8] M. Malekzadeh and M. T. Swihart, "Vapor-phase production of nanomaterials," *Chemical Society Reviews*, 2021.
- [9] D. Krishna, M. Sasikala, and V. Ganesh, "Adaptive FLC-based UPQC in distribution power systems for power quality problems," *International Journal of Ambient Energy*, pp. 1-11, 2020.
- [10] A. Sohani, S. Hoseinzadeh, and K. Berenjkar, "Experimental analysis of innovative designs for solar still desalination technologies; an in-depth technical and economic assessment," *Journal of Energy Storage*, vol. 33, p. 101862, 2021.
- [11] A. Kabeel, M. Abdelgaied, and G. Mahmoud, "Performance evaluation of continuous solar still water desalination system," *Journal of Thermal Analysis & Calorimetry*, vol. 144, no. 3, 2021.
- [12] E. Himabindu and M. G. Naik, "Energy Management System for grid integrated microgrid using Fuzzy Logic Controller," in *2020 IEEE 7th Uttar Pradesh Section International Conference on Electrical, Electronics and Computer Engineering (UPCON)*, 2020: IEEE, pp. 1-6.
- [13] M. Elashmawy, M. Alhadri, and M. M. Ahmed, "Enhancing tubular solar still performance using novel PCM-tubes," *Desalination*, vol. 500, p. 114880, 2021.
- [14] H. B. ELURI and M. G. Naik, "Challenges of RES with Integration of Power Grids, Control Strategies, Optimization Techniques of Microgrids: A Review," *International Journal of Renewable Energy Research (IJRER)*, vol. 11, no. 1, pp. 1-19, 2021.
- [15] A. A. Bachchan, S. M. I. Nakshbandi, G. Nandan, A. K. Shukla, G. Dwivedi, and A. K. Singh, "Productivity enhancement of solar still with phase change materials and water-absorbing material," *Materials Today: Proceedings*, vol. 38, pp. 438-443, 2021.
- [16] P. Boobalakrishnan *et al.*, "Thermal management of metal roof building using phase change material (PCM)," *Materials Today: Proceedings*, 2021.
- [17] C. Zhao, M. Opolot, M. Liu, F. Bruno, S. Mancin, and K. Hooman, "Phase Change Behaviour Study of PCM Tanks Partially Filled with Graphite Foam," *Applied Thermal Engineering*, p. 117313, 2021.
- [18] W. Drozd and M. Kowalik, "Technical and Cost Comparison of Selected Technologies for Energetic Conversions of Renewable Energy Sources," *Archives of Civil Engineering*, pp. 585-598-585-598, 2021.
- [19] ELURI, HIMA BINDU, and M. Gopichand Naik. "Challenges of RES with Integration of Power Grids, Control Strategies, Optimization Techniques of Microgrids: A Review." *International Journal of Renewable Energy Research (IJRER)* 11, no. 1 (2021): 1-19.
- [20] T. Sakagami, Y. Shimizu and H. Kitano, "Exchangeable batteries for micro EVs and renewable energy," *2017 IEEE 6th International Conference on Renewable Energy Research and Applications (ICRERA)*, 2017, pp. 701-705, doi: 10.1109/ICRERA.2017.8191151.
- [21] Bakiri, Hussein Abubakar, Hellen Maziku, Nerey Mvungi, Ndyetabura Hamisi, and Massawe Libe. "A Novel Load Forecasting Model for Automatic Fault

Clearance in Secondary Distribution Electric Power Grid using an Extended-Multivariate Nonlinear Regression." *International Journal of Smart Grid-ijSmartGrid* 5, no. 2 (2021): 103-112.

[22] Mesbahi, Oumaima, Mouhaydine Tlemçani, Fernando Manuel Janeiro, Abdeloawahed Hajjaji, and Khalid Kandoussi. "A Modified Nelder-Mead Algorithm for Photovoltaic Parameters Identification." *International Journal of Smart Grid-ijSmartGrid* 4, no. 1 (2020): 28-37.

[23] D. M. Ionel, R. De Doncker, A. Nasiri, Y. Nozaki and R. Miceli, "Keynote speakers: Plans for 100% renewable energy and requirements for technological developments," *2016 IEEE International Conference on Renewable Energy Research and Applications (ICRERA)*, 2016, pp. 11-15, doi: 10.1109/ICRERA.2016.7884351.